Ethylene Coordination, Insertion, and Chain Transfer at a Cationic Aluminum Center: A Comparative Study with *Ab Initio* Correlated Level and Density Functional Methods

GIOVANNI TALARICO,* PETER H. M. BUDZELAAR, ANTON W. GAL

Department of Inorganic Chemistry, University of Nijmegen, Toernooiveld 1, 6525 ED Nijmegen, The Netherlands

Received 27 August 1999; accepted 5 November 1999

ABSTRACT: The performance of correlated *ab initio* methods and DFT methods was compared for the propagation and chain transfer steps of ethylene polymerization by a model aluminum–amidinate system, $[\{HC(NH)_2\}AlCH_2CH_3]^+$. All methods agree that the main chain transfer mechanism is β-hydrogen transfer to the monomer (BHT), and that this is substantially *easier* than propagation; implications for the real Jordan system are discussed briefly. Counterpoise corrections are necessary to obtain reasonable olefin complexation energies. Activation energies are consistently lower at DFT (BP86, B3LYP) than at *ab initio* levels [MP2, MP3, MP4, CI, CCSD(T)]; the differences are particularly large (16 kcal/mol) for the BHT reaction. This is suggested to be related to the known problem of DFT in describing hydrogen bridged systems. J Comput Chem 21: 398–410, 2000

Correspondence to: G. Talarico, Dipartimento di Chimica, Università di Napoli, Via Mezzocannone 4, 80134, Naples, Italy; e-mail: talarico@chemna.dichi.unina.it

*G.T. thanks the University of Naples for a grant which allowed him to stay at the University of Nijmegen. We thank the Dutch Polymer Institute for providing part of the funding for purchasing our computers.

Contract/grant sponsors: University of Naples and the Dutch Polymer Institute

This article includes Supplementary Material available from the authors upon request or via the Internet at ftp.wiley.com/public/journals/jcc/suppmat/21/398 or http://journals.wiley.com/jcc/

Keywords: quantum chemical methods; aluminum; ethylene polymerization; DFT; CCSD(T)

Introduction

In the last few years intense theoretical and experimental activity has centered around homogeneous Ziegler–Natta catalytic systems, following the discovery of a highly active homogeneous metallocene catalyst[1] for olefin polymerization. Subsequently, not only early transition metal d^0 and lanthanide d^0f^n complexes[2] but also complexes of late transition metals such as Fe(II),[3] Co(II),[4] Ni(II), and Pd(II)[5,6] have been the subject of experimental and theoretical studies.[7] Experimental results suggested that in the case of zirconocene[8,9] and titanocene[10] catalysts the active species are cationic and monomeric. Various quantum mechanics calculations have assessed the widely accepted Cossee mechanism[11] as a viable one for the chain growth reaction. This mechanism involves π-coordination of the olefin to the active species followed by insertion of the olefin into the metal–alkyl bond through a four-center transition state. Although the intermediacy of a π-complex is widely accepted, one should keep in mind that there is no experimental proof of the existence of a discrete π-complex intermediate for early transition metal systems; some calculations suggest that the potential well around the π-complex can be exceedingly shallow for metallocene catalysts.[12]

A number of *ab initio*[12–14] and density functional theory methods[7] have been employed in studies of the electronic factors involved in the Cossee mechanism. Comparison of the results obtained with *ab initio* and density functional studies indicate that the Hartree–Fock method overestimates the olefin insertion barriers.[12,13] Inclusion of electron correlation effects was found to be very important in obtaining more accurate energetics.[12] For the energetics of ethylene insertion at group 4 metallocene catalysts only small discrepancies were found between correlated *ab initio* methods and density functional studies.[12,13c,14] It is interesting to note that no such comparisons have been reported for chain transfer processes. Several DFT studies have been reported,[15] but we know of only one study using a method other than DFT to investigate chain transfer reactions.[14]

Mono(amidinate) complexes of aluminum, $\{R^2C(NR^1)_2\}AlR_2$ (I), which react with $B(C_6F_5)_3$ to yield the cationic mono (II) and dinuclear aluminum alkyls (III), have been described recently[16] (Scheme 1).

According to Jordan,[16] monomeric compounds of type (II) are active species in ethylene polymerization, and are the first well-defined main group metal olefin polymerization catalysts. The formation of cationic species (II) and the related catalytic activity can be tuned by modifying the steric properties of the ligands through variation of R^1 and R^2. In particular, $\{R^2C(NR^1)_2\}AlR_2$ (I), with bulky substituents (R^2 = *tert*-butyl or methyl; R^1 = isopropyl) and $B(C_6F_5)_3$ as activator, shows a high molecular weight and a narrow molecular weight distribution in ethylene polymerization. These data are consistent with the hypothesis of a single-site catalyst with a high $k_{\text{chain-growth}}/k_{\text{chain-transfer}}$ ratio.[16a]

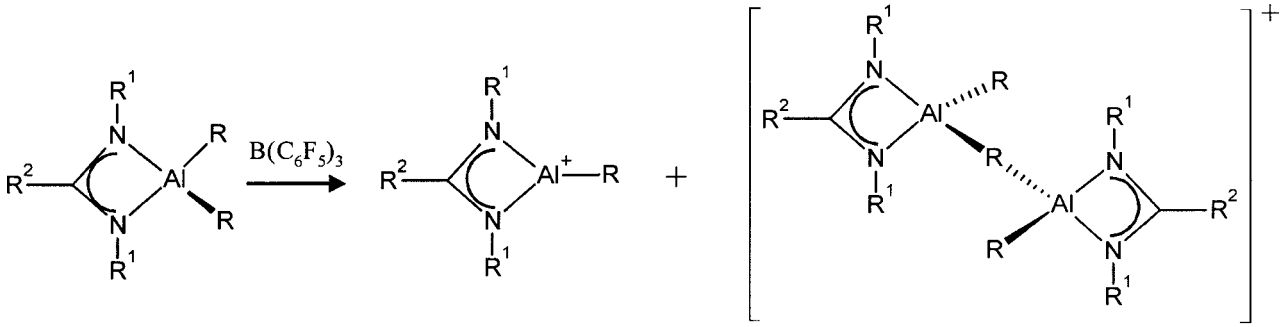

SCHEME 1.

There is some controversy about this Al system, because of the widespread belief that a transition metal is needed for efficient polymerization, even though the simple neutral aluminum alkyls, AlR_3, have long been known to be active in ethylene polymerization.[17] The activation energies for cationic aluminum species are expected to be larger than for the better known cationic d^0-transition metal systems.[14, 15] This makes the present Al system a nice model for studying electronic and steric ligand effects and specifically for comparing different computational methods.

In the present article, we aim to understand the mechanistic processes at the cationic Al center during the polymerization process. In particular, we want to establish what the relevant chain transfer mechanisms are, and we want to compare DFT and *ab initio* methods for both propagation and chain-transfer steps.

We chose unsubstituted (II) with R^1 and $R^2 = H$ as a simplified model. The growing chain was simulated by an ethyl group ($R = C_2H_5$) because the methyl group cannot be used to investigate some important chain termination paths. For the chain transfer process in transition metal catalyzed polymerization a number of different mechanisms have been suggested on the basis of experimental[18] and theoretical[14, 15] studies. Here, we consider three mechanisms: β-hydride elimination (BHE), β-hydrogen transfer to the monomer (BHT), and hydrogen transfer from the monomer to the alkyl chain by C—H activation (CHT). Two other termination processes that have been reported, β-alkyl elimination[19] and chain transfer to a cocatalyst,[20] are not relevant to the Jordan system and will not be considered here.

For these reaction paths we compared a density functional method with nonlocal corrections (BP86),[21, 22] a self-consistent hybrid method that includes density gradient correction and some Hartree–Fock exchange (B3LYP);[23] Hartree–Fock calculations (HF), and Møller–Plesset perturbation theory (MP2).[24] In addition, improved energies at the MP2 geometries were obtained by using higher order Møller–Plesset perturbation theory (MP3 and partial MP4),[25, 26] configuration interaction (CISD),[27] and a coupled cluster model [CCSD(T)].[28]

The basis set superposition error[29, 30] was evaluated for ethylene coordination energies at all levels of calculation and free energies for the transition states of insertion and chain transfer were computed. We neglected the role of the counter ion and solvent. The geometries of intermediates and transition states proved generally similar among the different computational methods, but a few significant differences exist. The potential energy profiles of ethylene insertion vs. chain termination were compared for the theoretical methods used. Meier et al.[31] recently reported a theoretical study of ethylene insertion at aluminum using the model system $[\{MeC(NMe)_2\}AlMe]^+$. That study was carried out only at the DFT level (using Car–Parrinello techniques[32]), and chain transfer was not considered.

Computational Methods

Geometries were optimized at four different levels: HF, MP2, B3LYP, and BP86. We did not impose any symmetry restrictions. The 6-31G(d) basis set[33] was used for the first three methods.

Pure density functional calculations were carried out with the ADF program.[34] The VWN exchange–correlation potential[21] was used in combination with Becke–Perdew nonlocal corrections.[22] This corresponds to the DFT level used for several transition metal olefin polymerization studies reported in refs. 7c, 7d, and 15. The usual acronym for this functional is BP86. A double-ζ+polarization[35, 36] basis (basis set III of the ADF program[34]) was used for Al, C, N, and H; the inner shells on the metal (up to 2p) as well as nitrogen and carbon (1s) were treated with the frozen core approximation.

For the MP2 calculations, all electrons were included in excitation lists, and no frozen core approximations were applied. Configuration interaction calculations including singles and doubles levels of theory (CISD)[27] with the Pople size consistency correction[37] were performed at MP2 optimized geometries. All these calculations were computed with the GAMESS-UK program.[38]

On the MP2 optimized structures we performed single-point calculations at the Møller–Plesset third-order (MP3)[25] and partial fourth-order [MP4(D), MP4(DQ) MP4(SDQ)][26] levels. For obtaining the best correlation-corrected energy values, a single-reference coupled cluster model including single, double and a perturbative estimate of triple excitations, CCSD(T),[28] was used for all MP2 optimized geometries. CCSD(T) energies computed for the BP86 optimized geometries were found to be virtually the same (less than 0.3 kcal/mol higher), and thus omitted. The frozen core approximation was used after having checked that the relative energies obtained coincide with those of the all-electron calculations. For the CCSD(T) calculations, the default SCF convergence criterion was found to be

inadequate, and "Scf=Tight" had to be used. Energy calculations at the MP2 level of theory were also carried out with larger basis sets: 6-31G(d,p), 6-311G(d,p), and 6-311G(2d,p).

The nature of each stationary point was characterized by computing the harmonic vibrational frequencies. For some important structures a zero-point correction and a thermodynamic correction for temperature effects were also evaluated (HF frequencies were scaled by 1/1.12[39]). All these calculations were done with the GAUSSIAN94 program.[39]

GAUSSIAN94 was also used to calculate geometries and energies with the hybrid density functional method B3LYP.[23] This method consists of a Becke gradient correction to exchange[22a] and Lee–Yang–Parr[23a] correlation functional, and corresponds to the methods used in refs. 7a and 7b.

Counterpoise corrections (CP) for the basis set superposition error (BSSE) were evaluated for olefin complexes according to the Boys–Bernardi method.[13c, 40] CP corrections were evaluated with ADF (for BP86 calculations) and GAUSSIAN94 (for all other methods).

Geometries

We first discuss the geometries of the optimized structures at the MP2 level. The structures for the ethylene reaction pathways at the cationic Al center are shown in Figure 1. The main geometrical parameters obtained by optimization with HF, MP2, BP86, and B3LYP calculations are listed in Table S-I of the Supplementary Material. As a measure of nonplanarity around the Al center in $[LAlX]^+$ (X = H, Et, Bu) we used the angle $\theta = \angle$ C—Al—Y, where C is the carbon of the amidinate backbone and Y = H or C.

ETHYLENE COORDINATION

The cationic species $[LAlC_2H_5]^+$ (**1**) shows a trigonal planar structure with the C_α—C_β bond lying in the L–Al plane. Rotation around the Al—C_α bond is nearly free with energy differences about 0.1–0.3 kcal/mol at the MP2 level. Because of a weak agostic interaction, perhaps more properly called hyperconjugation, both C_α—H_α bonds are slightly elongated (1.098 Å) compared to a normal C—H bond (1.092 Å). The distance Al–C_α is 1.929 Å, with an angle Al—C_α—C_β of 114.1°. Due to the trigonal planar structure, the β-hydrogen atoms do not show any significant interaction with the Al center.

In ethylene complex (**2**) the ethylene is coordinated relatively weakly. The ethylene–Al distance (2.357 Å) is quite long, and the ethylene C_1—C_2 bond (1.353 Å) is only slightly longer than in the free molecule (1.336 Å). The Al–C_α distance (1.935 Å) is hardly elongated compared to that in precursor **1**. However, rotation of the ethyl-chain locates the C_β atom in position "trans" to the coordinated ethylene in order to accommodate the olefin. The preferred coordination for the ethylene is with $H_2C{=}CH_2$ perpendicular to the Al—R bond, but parallel coordination is only 1 kcal/mol higher in energy. Thus, ethylene rotation is nearly free.

Following the ethylene coordination, there are three possible reaction pathways: chain growth via ethylene insertion (**TS 3**), or chain transfer either via β-H transfer to ethylene (**TS 5**) or via H transfer from the monomer to ethyl chain (**TS 6**).

ETHYLENE INSERTION

From π-complex **2** the reaction proceeds through the four-centered transition state (**TS 3**), after a 90° ethylene rotation.

From the analysis of **TS 3** in Figure 1 we observe that the Al—C_1 σ-bond (1.984 Å) is nearly formed, and the Al—C_α bond (2.062 Å) is elongated; this would suggest that **TS 3** is a late transition structure. The olefin bond length (C_1—C_2) has increased from 1.353 to 1.439 Å. The C_α–C_2 distance is 2.213 Å; this is still much longer than a typical C—C single bond (1.541 Å), suggesting an early transition state. Thus, the reaction appears to be concerted but nonsynchronous. The four-membered ring is nearly planar, with a dihedral angle Al—C_1—C_2—C_α = 9.2° and may be stabilized by a weak α-agostic interaction[41] (C_α—H_α = 1.109 Å; Al—H_α = 2.220 Å). The ethyl chain has rotated out of the plane to minimize steric interactions with the ethylene.

Structure **4** is the primary product of the ethylene insertion, with the resulting *n*-butyl chain in the most stable conformation. The presence of a γ-agostic interaction is obvious from the short Al–H_γ distance (2.126 Å) and the elongated C_γ—H_γ bond (1.125 Å). The calculations show that there are β-agostic *n*-butyl conformations, which are slightly higher in energy. This is remarkable, because in transition metal systems β-agostic interactions are usually the strongest ones. For aluminum systems, distortion of the coordination geometry away from a trigonal structure and of the M—C—C angle away from a tetrahedral geometry at C_α, are more difficult than for transition metal complexes. Therefore, only agostic interactions that can form without geometric deformations are favorable. This excludes α- and β-agostic structures.

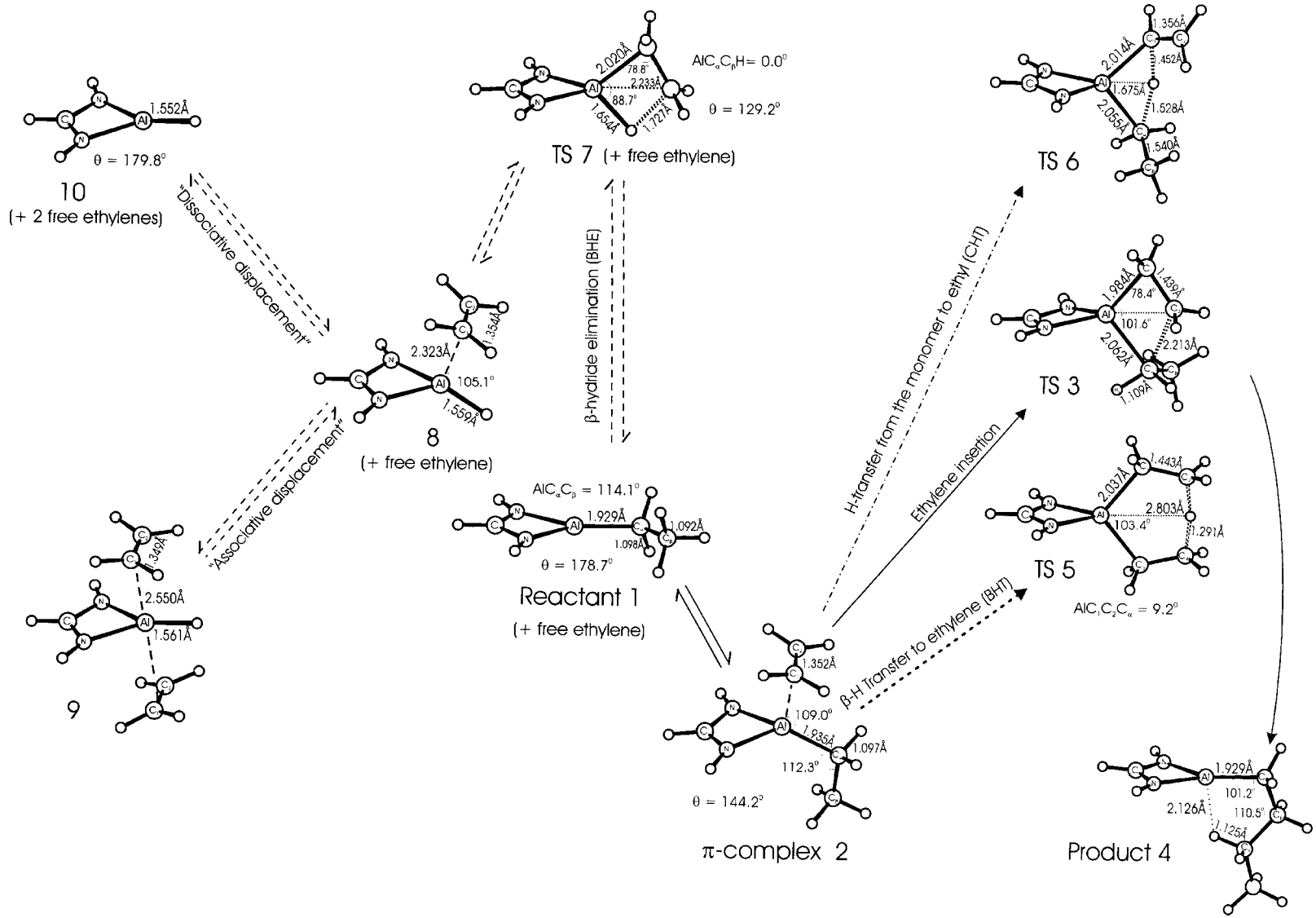

FIGURE 1. MP2 optimized structures for stationary points in the $[\{HC(NH)_2\}AlEt]^+ + C_2H_4$ system: reactant **1**, π-complex **2**, ethylene insertion **TS 3**, γ-agostic product **4**, β-hydrogen transfer to the monomer (BHT) **TS 5**, hydrogen transfer from the monomer to the alkyl chain by C—H activation (CHT) **TS 6**, β-hydride transfer to the metal (BHE) **TS 7**, hydride–olefin π-complex **8**, hydride-bis(ethylene) π-complex **9**, and "naked" metal hydride**10**. Bond lengths in Angstroms, angles in degrees.

β-HYDROGEN TRANSFER TO ETHYLENE (BHT)

The transition structure for BHT (**TS 5**) has C_{2v} symmetry with the H atom equidistant from two ethylene fragments (1.291 Å). The Al–C distances are only slightly larger than for Al—C σ bonds (2.037 Å, compared to 1.929 Å); the C–C distance of 1.443 Å is intermediate between that of a single and a double bond. The long Al–H distance (2.803 Å) indicates the absence of a direct Al–H interaction, and is in marked contrast to the M–H interaction in the corresponding transition structures for transition metal catalysts. In fact, calculations based on density functional methods[15c, 15d] stressed that, for the $[Cp_2ZrEt]^+ + C_2H_4$ TS, the M–H distance (1.96 Å) in the transition state is close to a bonding distance, thus indicating participation of the metal center in the β-H transfer process.

HYDROGEN TRANSFER FROM ETHYLENE TO ETHYL (CHT)

Another termination reaction that we have considered involves the activation of a C—H σ bond of the monomer. In this reaction the ethylene approaches the metal center with a C—H bond (**TS 6**). One H atom is transferred from the olefin to the polymer chain, resulting in ethane and an aluminum vinyl species $[LAl—CH=CH_2]^+$.

The four-centered transition structure shows an H atom almost half-way between the vinyl (H—C_1 = 1.452 Å) and the ethyl fragment (H—C_α = 1.528 Å). The olefin C_1—C_2 bond is 1.356 Å, which is very close to the value for a double bond, and the Al—C_α and Al—C_1 distances are similar (2.055 and 2.014 Å, respectively). A weak σ-agostic interaction is present as indicated by a short Al–H_α distance (2.419 Å) and a slightly elongated C_α—H_α bond (1.104 Å). Finally, the Al–H distance (1.675 Å) is only 0.116 Å longer than in Al hydride complex **8** (Fig. 1). Compared to **TS 5**, the structure **TS 6** indicates some metal assistance in the H transfer to the alkyl chain. This assistance affects the charge at H (vide infra).

β-HYDRIDE ELIMINATION (BHE)

This reaction starts from **1** and goes via the four-centered transition state (**TS 7**), producing an $[LAl—H]^+$ coordinated ethylene. At the corresponding transition structure (**TS 7**) the distance Al–C_α is only slightly elongated (2.020 Å compared to 1.929 Å) but the Al—H bond is already formed (1.654 Å), while the C_2—H bond is almost broken (1.727 Å); the C_1–C_2 distance has become 1.421 AA, close to a double bond. The considerable amount of Al—H bond formation and C—H bond breaking, indicates the "product-like" nature of **TS 7**.

In product **8**, an ethylene is coordinated to an Al–hydride in a pseudotetrahedral structure with Al—H bond (1.559 Å) bent out of the ligand plane ($\theta = 145°$). The ethylene molecule is weakly coordinated to the metal center (Al–olefin = 2.323 Å) and oriented perpendicular to the Al—H bond. Overall, **8** resembles alkyl–ethylene complex **2**, but the smaller size of the hydrogen has led to a somewhat smaller Al–ethylene distance.

Ethylene dissociation from **8** to give "naked" $[LAl—H]^+$ (**10**) is highly endothermic (see next section). The association of a second ethylene, however, converts **8** to a stable five-coordinated bis(ethylene)-aluminum–hydride complex $[LAlH(C_2H_4)_2]^+$ (**9**). The symmetric complex **9**, obtained through full optimization from an asymmetrical starting geometry, is a local minimum according to normal mode analysis. There may be other stable conformations with different orientations of the ethylenes, but they are expected to have very similar energies. The two olefin molecules are only weakly bound, as demonstrated by the ethylene double bond distance (1.349 Å) and the large Al–olefin distance (2.550 Å).

COMPARISON OF THE OBTAINED GEOMETRIES

It is nowadays well established that DFT based methods, either "pure" DFT with nonlocal corrections or hybrid HF-DFT calculations, provide geometrical parameters that are close to those obtained by the MP2 approach.[42] In our studies, the intermediates and transition structures showed very similar geometries at HF, MP2, B3LYP, and BP86 level. Nevertheless, from Table S-I we note that MP2 calculations predict "bonding" distances to be shorter than BP86. This is particularly clear in the weakly bound ethylene complexes (**2**, **8**, and **9**), in which the metal–ethylene distances are 0.05 to 0.10 Å shorter at the MP2 level. The shortening of the Al–ethylene distance, however, does not correspond to a lengthening of the olefin C—C bond; this bond is always shorter at MP2 level. We suggest that the shorter Al–ethylene distances in MP2 geometries are an artifact caused by a much larger BSSE at MP2 than at BP86 level, as discussed later on. Nonbonded distances do not show any obvious trend.

Energetics

To give a quick overview of the potential energy surface, the overall MP2 energy profile is plotted in

Figure 2. Before discussing the full profile, we need to consider that for ethylene binding at metal centers as in **2**, **8**, or **9**, the energy values are affected by the basis set superposition error,[29] thus leading to an overestimation of the binding energies. The correct handling of BSSE in geometry optimization studies is not trivial.[30] This may be one of the reasons why it was neglected in most articles on the olefin polymerization. Counterpoise correction[40] can only be applied to systems that can be unambiguously divided into independent molecules. This applies to ethylene complexes (**2**, **8**, and **9**), but clearly not to the transition structures (**TS 3**, **TS 5**, **TS 6**, and **TS 7**) or to the product (**4**) (see ref. 13c). In this article, we assume that, from the olefin complex stage onward, the BSSE remains constant over the reaction path. In any case, the CP correction to the complexation energy should generally be too low, because the artificial attraction caused by BSSE will force the system into the repulsive region of the potential energy surface.

ETHYLENE COORDINATION

As discussed above, the ethylene complexation energy is contaminated by the BSSE. The values obtained by the various calculations without CP correction show a large spread (18–25 kcal/mol), but they move much closer upon CP correction (16–19 kcal/mol), with the exception of CI calculations (13 kcal/mol)[43] (see Table I, third column). The CP correction increases upon going from the HF level (2 kcal/mol) to the MP2 level, for which it is quite large[13c, 44] (6 kcal/mol). For BP86 and B3LYP, it is about the same as for HF, ca. 2 kcal/mol. This supports our suggestion that the BSSE cannot be ignored when comparing computational methods. The better basis sets decrease the CP correction somewhat but do not change the corrected Al–ethylene complexation energy significantly (Table S-II). The large binding energy of ethylene can be accounted for by considering the strong interaction of the coordinatively unsaturated, positively charged Al complex with the π-bonding orbital of ethylene. It should be noted here that in solution a solvent molecule would be coordinated to the vacant coordination site; this will decrease the effective ethylene binding energy.

ETHYLENE INSERTION

The calculated activation energies for olefin insertion (Table I, fourth column) confirm that insertion at an aluminum center is more difficult than at early transition metal d^0 centers.[15a–c] All the post-HF methods predict a barrier of 30–33 kcal/mol; apparently the Møller–Plesset perturbation series is sufficiently converged at MP2. The HF method predicts higher energies of 38 kcal/mol, as expected.[12–14] Lower barriers are obtained with

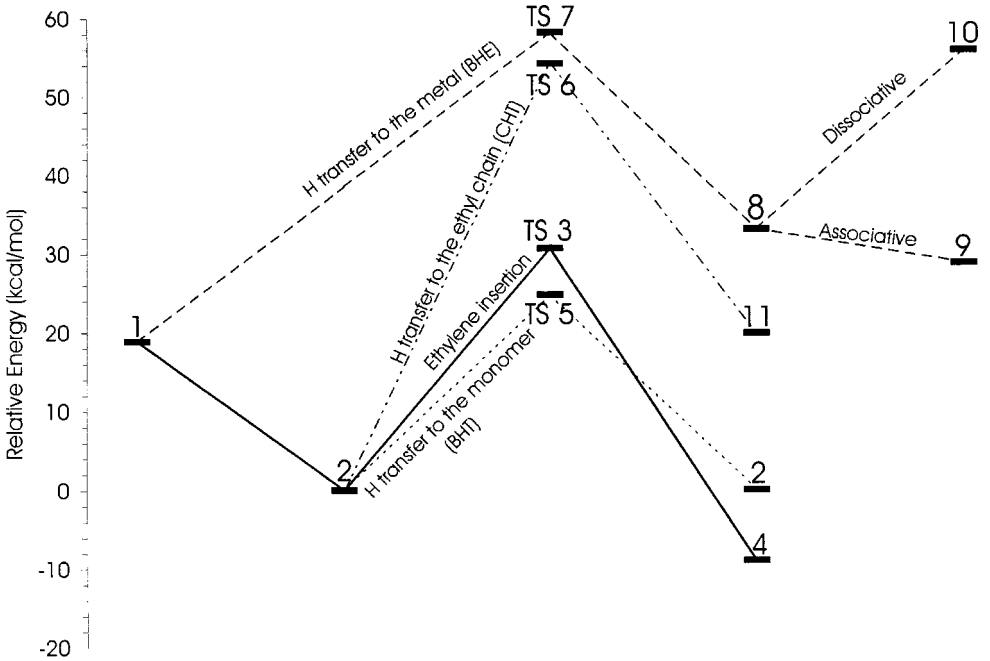

FIGURE 2. Reaction profile at MP2 level.

TABLE I.
Method Dependence of Olefin Coordination and Insertion; Energies Relative to π-Complex $[HC(NH)_2AlCH_2CH_3(CH_2CH_2)]^+$ (kcal/mol).

Method	E_{BSSE}	Reactant **1**[a] (Complexation)	**TS 3** (Insertion)	Product **4**
BP86	2.9	15.9	23.0	−9.7
B3LYP	2.6	17.7	27.6	−8.2
HF	2.0	15.9	37.6	−7.6
CI	4.2	13.3	32.7	−8.7
MP2	6.1	18.9	30.6	−9.0
MP3	5.0	17.9	33.0	−8.5
MP4(D)	5.0	17.7	33.1	−8.0
MP4(DQ)	4.8	17.3	33.6	−8.5
MP4(SDQ)	4.7	17.3	32.7	−8.2

[a] Corrected for BSSE.

density functional methods: 23 kcal/mol for BP86, and 28 kcal/mol for B3LYP. These discrepancies are quite surprising, because they do not correspond to significant differences in transition state geometries (see Table S-I). Additionally, Jensen and Børve have shown recently that density functional theory (BP86) gives results in excellent agreement with *ab initio* correlated levels for ethylene insertion at $[H_2TiCH_3]^+$.[45] Our BP86 value for the insertion barrier is in line with the recent results by Meier et al.[31] for $[\{MeC(NMe)_2\}AlMe]^+$ (25 kcal/mol). These authors also estimated a much higher barrier for insertion into a methyl bridged dinuclear species (see III in Scheme 1), suggesting that the monomeric species is the active catalyst.

Basis set effects on the barrier are small: using a 6-311G(2d,p) basis set, the transition state energy is lowered by 2 kcal/mol at the MP2 level (Table S-II).

The overall reaction of ethylene insertion into **1** yielding the final structure **4**, is exothermic by 22–27 kcal/mol for all calculations after CP correction. These data are in line with an estimate of 20–25 kcal/mol based on the formation of two C—C single bonds from one C=C double bond;[46] without CP correction, the agreement is not as good (24–33 kcal/mol).

β-HYDRIDE ELIMINATION (BHE)

The energetics for this chain transfer process (Fig. 1) are reported in Table II. The (high) barrier in going from **1** to transition structure **TS 7** is similar for all *ab initio* correlated techniques (39 kcal/mol). The HF value is also close, indicating that in this case the electron correlation does not play an important role. A lower barrier is calculated with BP86 (32 kcal/mol) and an intermediate value with B3LYP (35 Kcal/mol). The barriers from the various computational methods reproduce the same trend as for ethylene insertion into the Al—ethyl bond: BP86 < B3LYP < *ab initio* correlated < HF.

The reaction path leading to product **8** is endothermic by about 15 kcal/mol. Displacement of the coordinated olefin from **8** to complete the chain transfer reaction could occur in two different ways. Dissociative displacement to give **10** is highly endothermic (20–22 kcal/mol above **8**, 32–38 kcal/mol above **1**, see Table II); but under conditions where **TS 7** is accessible, **10** should also be accessible. In the presence of free olefin, however, associative dis-

TABLE II.
Energies of β-Hydrogen Transfer to the Metal (BHE) Relative to Precursor $[HC(NH)_2AlCH_2CH_3]^+$ (kcal/mol).

Method	**TS 7** (BHE)	Structure **8**	Structure **9**[a]	E_{BSSE}[b]	Structure **10**[a]	E_{BSSE}[c]
BP86	32.0	16.1	11.7	2.2	36.5	2.3
B3LYP	34.9	15.0	11.1	2.4	37.7	2.5
HF	39.3	12.8	11.7	1.8	33.0	2.0
CI	38.9	13.5	15.8	3.6	31.7	4.0
MP2	39.2	14.1	9.9	5.2	36.9	5.8
MP3	39.5	13.9	11.1	4.3	35.9	4.7
MP4(D)	39.3	13.3	10.4	4.3	35.0	4.7
MP4(DQ)	39.7	13.9	11.6	4.2	35.2	4.5
MP4(SDQ)	38.8	13.6	11.1	4.1	34.9	4.5

[a] Corrected for BSSE.
[b] Relative to **9**.
[c] Relative to **8**.

placement via bis-olefin complex **9** is much easier: **9** is slightly below **8**, by 1 kcal/mol at HF, and by 3–4 kcal/mol at all other levels. The CP corrections for **9** are similar to those for **8**.

The reverse barrier, corresponding to ethylene insertion into the aluminum—hydride bond (**8** → **TS 7**), is 16–25 kcal/mol, depending on the approach used. Comparison with the barriers for **2** → **TS 3** (23–38 kcal/mol) shows that insertion of ethylene into an Al—hydride bond is much easier than into an Al—ethyl bond. One reason is that the Al—ethyl bond is much more directional than the Al—hydride bond, due to the presence of a C sp^3 hybrid orbital instead of nondirectional H s orbital. Therefore, the metal—carbon bond has to be essentially broken before the alkyl group can start to bind to the olefin. This observation is in agreement with the relative insertion rates measured experimentally for neutral scandocene alkyl and hydride complexes.[47]

For MP2, extended basis sets result in a lower CP correction and a slightly lower ethylene coordination energy (Table S-III).

HYDROGEN TRANSFER FROM ETHYLENE TO ETHYL (CHT)

This reaction has a high activation energy, comparable to that of β-hydride elimination (Table III). Again, BP86 and B3LYP give lower barriers than *ab initio* correlated levels. The influence of the basis set at the MP2 level is remarkable. In fact, using an extended basis set, the MP2 energy value becomes similar to the B3LYP value (Table S-IV). After CHT a $[LAl–vinyl]^+$ species is formed, which might start a new chain with a vinyl head group. The product of CHT (not shown in Fig. 1) is less stable than **2** (by about 15–20 kcal/mol at all levels of calculations) because it lacks the stabilizing Al–olefin complexation.

β-HYDROGEN TRANSFER TO ETHYLENE (BHT)

BHT (via **TS 5**) turns out to have the lowest barrier energy of all chain-transfer processes considered here. When we compare it with CHT (**TS 6**) and BHE (**TS 7**) (Table III), we see that is lower by ~30 kcal/mol at all levels considered. Remarkably, the activation barrier for BHT is smaller than the one calculated for the ethylene insertion. *Thus, all calculations predict that the present model system would not polymerize ethylene!*

The energy values obtained with density functional theory (BP86 as well as B3LYP) differ significantly from the ones obtained with post-HF methods. It is particularly surprising that BP86 gives an extremely low barrier for BHT (only 9 kcal/mol) relative to the *ab initio* correlated methods (25–28 kcal/mol). This results in a much larger gap between chain growth and chain transfer than obtained with *ab initio* methods. The last column of Table III shows the resulting differences between propagation and termination at the various levels.

Studies by Ziegler[15b] have demonstrated that free-energy calculations can be necessary to obtain a correct balance between propagation and chain transfer. Therefore, we performed a thermal analysis based on frequency calculations.

The entropy and energy contributions[48] for **TS 3** and **TS 5** are summarized in Table IV. For conciseness, we report only the data obtained at HF level. Nearly identical results (within 1 kcal/mol)

TABLE III.
Method Dependence of Activation Energies (Relative to $[HC(NH)_2AlCH_2CH_3(CH_2CH_2)]^+$) in (kcal/mol).

Method	TS 3 (Insertion)	TS 5 (BHT)	TS 6 (CHT)	TS 7[a] (BHE)	$\Delta E_{\text{chain growth-chain transfer}}$
BP86	23.0	9.1	41.0	48.5	13.9
B3LYP	27.6	16.5	49.4	52.6	11.1
HF	37.6	33.7	65.7	55.2	3.9
CI	32.7	27.7	57.5	52.2	5.0
MP2	30.6	24.7	54.1	58.1	5.9
MP3	33.0	28.0	57.0	57.4	5.0
MP4(D)	33.1	28.2	56.9	57.0	4.9
MP4(DQ)	33.6	28.9	57.8	57.0	4.7
MP4(SDQ)	32.7	27.4	57.2	56.2	5.3

[a] Corrected for BSSE.

TABLE IV.
Thermodynamic Data for the Barriers for Ethylene Insertion and H-Transfer to the Monomer with the π-Complex (Structure 2) as a Reference, Calculated at HF Level.

	TS 3 (Insertion)	**TS 5** (BHT)
ν_{IMAG} [cm^{-1}]	550.8i	917.8i
ΔS_{trans} [cal/mol-K]	0.00	0.00
ΔS_{rot} [cal/mol-K]	−0.33	−0.18
ΔS_{vib} [cal/mol-K]	−12.35	−11.96
ΔS_{tot} [cal/mol-K]	−12.69	−12.15
ΔH_{ZPC} [kcal/mol]	0.2	−2.2
ΔH_{trans} [kcal/mol]	0.00	0.00
ΔH_{rot} [kcal/mol]	0.00	0.00
ΔH_{vib} [kcal/mol]	−1.2	−1.1
ΔH_{tot} [kcal/mol]	−1.0	−3.3
ΔG [kcal/mol] (298.15 K)	**2.8**	**0.3**

were obtained from frequency analyses at BP86 and B3LYP levels.

Both transition structures show a negative entropy of activation mainly due to a decreased vibrational entropy relative to π-complex **2**. The nearly free ethylene rotation in **2** is frozen out in compact transition structures **TS 3** and **TS 5**. The zero-point energy correction (ΔH_{ZPC}) is virtually zero for propagation, but lowers the chain transfer barrier by 2 kcal/mol. In the final analysis the free energy of activation (ΔG) is increased by 2.8 kcal/mol for the insertion of ethylene via **TS 3**, and by 0.3 kcal/mol for the β-H transfer to ethylene via **TS 5**. Because H-transfer to ethylene is the prevalent chain termination, it corresponds to an increase of the difference between chain transfer and chain growth.

We recall that the process is studied *in vacuo*, and that the inclusion of solvent effect will raise the free energy of activation due to solvent friction. It is difficult to predict whether this effect will be different for chain propagation and chain termination. Considering the small magnitude of this correction, it is clear that, at least for the simple model considered here, chain transfer reaction will always be preferred to chain propagation.

Energetics at the CCSD(T) Level

In an attempt to clarify the observed disparities between the energy values of *ab initio* and density functional methods, we performed single point calculations at the CCSD(T) level, which is probably the most reliable level available to us for a system of this size. CCSD(T) calculations have frequently been used as a "benchmark" to check the quality of *ab initio* and DFT calculations.[45] It turns out to be useful to consider olefin complexation separately from the various transition states. In Tables V and VI the ethylene coordination energies and the activation energies are compared with those obtained at BP86, B3LYP, and MP2 levels.

TABLE V.
Energies of Ethylene Coordination to Al-Hydride and Alkyl Species (kcal/mol).[a]

Method	$\Delta E_{1\rightarrow 2}$	$\Delta E_{8\rightarrow 9}$	$\Delta E_{10\rightarrow 8}$
BP86	−15.9	−4.4	−20.4
B3LYP	−17.7	−3.9	−22.7
MP2	−18.9	−4.2	−22.8
CCSD(T)	−17.6	−3.1	−21.9

[a] Corrected for BSSE.

The scatter in calculated ethylene coordination energies among different methods appears to be insignificant (less than 3 kcal/mol). The situation is more interesting for the activation energies in Table VI. The results at the CCSD(T) level essentially agree (within 1–2 kcal/mol) with the MP2 results, and differ significantly from those obtained with BP86 (and to a lesser extent B3LYP). We already noted that in order to obtain accurate energies for CHT (**TS 6**), a better basis set is needed at the MP2 level (Table S-IV); this is probably also true for CCSD(T). For the other reactions, however, basis set effects are small, and cannot be responsible for the observed differences. As CCSD(T) is the most accu-

TABLE VI.
Energies of Transition Structures TS 3, TS 5, TS 6, and TS 7 Obtained at Different Levels (kcal/mol).

Method	**TS 3**[a] (Insertion)	**TS 5**[a] (BHT)	**TS 6**[a] (CHT)	**TS 7**[b] (BHE)
BP86	23.0	9.1	41.0	32.0
B3LYP	27.6	16.5	49.4	34.9
MP2	30.6	24.7	54.1	39.2
CCSD(T)	31.5	25.4	55.4	37.2

[a] Relative to π-complex structure **2**.
[b] Relative to the reactant **1** + free ethylene.

TABLE VII.
Calculated Atomic Charges by Distributed Multipole Analysis (at MP2) for Important Atoms of All Species Mentioned in the Text.

	Atomic Charges					
Structure	Al	C_α	C_β	H	C_1	C_2
Reactant **1**	1.90	−0.74	0.17	0.12	—	—
π-complex **2**	1.94	−0.78	−0.15	0.09	−0.22	−0.22
TS 3	1.95	−0.65	−0.18	0.13	0.04	−0.71
Product **4**	1.89	−0.78	−0.04	−0.05	—	—
TS 5 (BHT)	2.04	−0.84	0.12	**−0.09**	−0.84	0.12
TS 6 (CHT)	1.97	−0.80	−0.15	**0.43**	−0.81	0.01
TS 7 (BHE)	1.92	−0.69	0.02	**−0.39**	—	—
Structure **8**	1.87	—	—	−0.50	−0.23	−0.23
Structure **9**	1.85	−0.22	−0.22	−0.55	−0.22	−0.22
Structure **10**	1.88	—	—	−0.41	—	—

The atom numbering scheme is $H_2C^1{=}CH_2^2$ for the olefin and Al—C_α—C_β—C_γ for the growing chain. The H atom in the table correspond to the H in α-position for the structures **1**, **2**, **TS 3**; in γ for the structure **4**; the H transferred in the termination processes BHT, CHT, BHE, and the H bonded to the metal for the structures **8**, **9**, and **10**.

rate method applied here, the lower BP86 barriers are alarming. The discrepancies vary in a nonsystematic way from 8 kcal/mol for ethylene insertion to 16 kcal/mol for BHT. The main consequence is a completely distorted ratio between ethylene insertion and chain transfer.

There are some literature reports that DFT methods overestimate the stability of transition structures in which a hydrogen atom is equally shared between two electronegative atoms.[49] In the case of **TS 5**, the hydrogen atom is shared between two carbon atoms, which are approximately of the same electronegativity as the hydrogen atom. A distributed multipole analysis reported in Table VII does not indicate a significant charge separation between C and H. So, our observations suggest that the reported problem might be more general. This drawback of pure DFT (BP86) is only partially reduced by using the hybrid density functional/Hartree–Fock approach B3LYP.

Table VII also contains a nice indication of differences in the nature of hydrogen transfer for three termination processes studied. In the CHT route (**TS 6**), the H atom being transferred has protonic character (charge 0.4), while in the BHT route (**TS 5**) a neutral hydrogen (charge −0.1) is transferred. Finally for BHE (**TS 7**), hydride character is indicated (charge −0.4). This also shows that the above mentioned DFT problem cannot be related to charge separation, else it would have been largest for CHT.

Conclusions

In the present article we investigated ethylene coordination, insertion, and chain transfer at a cationic Al center with various *ab initio* and density functional methods. We used the unsubstituted system $[\{HC(NH)_2\}AlCH_2CH_3]^+$ as a simplified model of the Jordan active species $[\{R^2C(NR^1)_2\}AlR]^+$.[16a] The following *chemical* conclusions can be drawn: (1) ethylene π-coordination to $[LAlEt]^+$ is highly exothermic (15–19 kcal/mol). Even higher coordination energies are found for ethylene π-coordination to $[LAlH]^+$ (20–22 kcal/mol). (2) The activation energy for ethylene insertion in the Al—Et bond is quite high (23–33 kcal/mol). Smaller barriers are obtained for ethylene insertion in the aluminum—hydride bond (16–25 kcal/mol). These values are considerably higher than the activation energy calculated for the ethylene insertion in the homogeneous system $Cp_2ZrCH_3^+$ (0.7 kcal/mol).[15a] (3) The prevalent chain termination mechanism is chain β-hydrogen transfer to the ethylene (BHT). The barriers for the other two termination mechanisms considered here—β-hydrogen transfer to the metal (BHE), and C—H σ-bond activation (CHT)—are so much higher (∼30 kcal/mol) that these reactions cannot occur. For BHT at aluminum, any direct interaction with the metal is absent. This should be contrasted with transition metal systems where, according to Ziegler,[15b, 15c] the associative displace-

ment transition state has a structure intermediate between that of direct chain transfer to the monomer and a $M(H)(C_2H_4)_2^+$ complex. (4) For all methods used the barrier for chain termination is (much) smaller than for ethylene insertion. *If the Jordan catalyst is indeed a monomeric cationic [(amidinate)Al-alkyl]$^+$species*, our results imply that the amidinate substituents do more than prevent the association to III in Scheme 1 (i.e., favoring the formation of mononuclear cationic species II):[16] they must *also* increase the rate of propagation relative to chain termination to obtain polymerization catalyst. We will address this issue in a forthcoming article.[50]

In addition some *methodological* conclusions can be drawn: (1) the counterpoise correction[40] for the basis set superposition error[29, 30] is necessary when comparing different computational approaches. In fact, the variation of the basis set superposition error among the computational methods (2 kcal/mol for BP86, B3LYP, or HF, but 6 kcal/mol for MP2) makes a counterpoise correction in the evaluation of ethylene binding necessary. The basis set 6-31G(d) adequately represents the geometries and energetics of these structures if used together with counterpoise correction. (2) *Ab initio* and density functional methods give different results for the energetics of ethylene polymerization by $[LAlEt]^+$. A clear trend for the activation energies was found: BP86 < B3LYP < *ab initio* correlated < HF. The discrepancies between BP86 and MP2 or CCSD(T) results vary nonsystematically from ca. 8 kcal/mol for the ethylene insertion to ca. 16 kcal/mol for chain termination. (3) For the first time a comparative study between *ab initio* correlated methods and approaches based on the density functional theory has been extended to the chain termination processes in olefin polymerization. The results are surprising, because the barrier obtained for the β-hydrogen transfer to the monomer with the DFT methods BP86 and B3LYP is too low. This problem appears to be related to the previously reported overestimation by DFT of the stability of structures containing an H bridge between electronegative atoms.[49] From our results, this drawback seems to be more general, and to occur also for transition state structures in which a hydrogen atom is shared between two carbon atoms. Thus, it might also be important in chain transfer at transition metal centers. It must, however, be noted here that the BHT transition state structure for aluminum is different from that for transition metal complexes,[15b–e] so a direct extrapolation from our results to transition metals is not possible.

Acknowledgments

The authors thank Dr. J. H. van Lenthe (University of Utrecht) for helpful discussions and generous amounts of computer time.

Supplementary Material

Tables of cartesian coordinates optimized at MP2 level and the total energies computed at CCSD(T) level of all species mentioned in the text and influence of basis sets (Tables S-I, S-II, S-III, and S-IV) are available as supplementary material from the *Journal of Computational Chemistry*.

References

1. Anderson, A.; Cordes, H. G.; Herwig, J.; Kaminsky, W.; Merk, A.; Motweiler, R.; Sinn, J. H.; Vollmer, H. J. Angew Chem Int Ed Engl 1976, 15, 630.
2. Brintzinger, H. H.; Fisher, D.; Mülhaupt, R.; Rieger, B.; Waymouth, R. M. Angew Chem Int Ed Engl 1995, 34, 1143.
3. Small, B. L.; Brookhart, M. J Am Chem Soc 1998, 120, 7143.
4. Small, B. L.; Brookhart, M.; Bennett, A. M. A. J Am Chem Soc 1998, 120, 4049.
5. Johnson, L. K.; Killian, C. M.; Brookhart, M. J Am Chem Soc 1995, 117, 6414.
6. Johnson, L. K.; Mecking, S.; Brookhart, M. J Am Chem Soc 1996, 118, 267.
7. (a) Musaev, D. G.; Froese, R. D. J.; Svensson, M.; Morokuma, K. J Am Chem Soc 1997, 119, 367; (b) Musaev, D. G.; Svensson, M.; Morokuma, K.; Stromberg, S.; Zetterberg, K.; Siegbahn, E. M. Organometallics 1997, 16, 933, and references therein; (c) Margl, P.; Deng, L.; Ziegler, T. Organometallics 1998, 17, 933; (d) Margl, P.; Deng, L.; Ziegler, T. J Am Chem Soc 1998, 120, 5517, and references therein; (e) Deng, L.; Margl, P.; Ziegler, T. J Am Chem Soc 1999, 121, 6479.
8. Alelyunas, Y. W.; Jordan, R. F. J Chem Educ 1988, 65, 285.
9. Yang, X.; Stern, C. L.; Marks, T. J. J Am Chem Soc 1991, 113, 3623.
10. Eisch, J. J.; Caldwell, K. R.; Werner, S.; Kruger, C. Organometallics 1991, 10, 3417.
11. (a) Cossee, P. J. Catal 1964, 3, 80; (b) Arlman, E. G.; Cossee, P. J. Catal 1964, 3, 99.
12. Weiss, H.; Ehrig, M.; Ahlrichs, R. J Am Chem Soc 1994, 116, 4919.
13. (a) Kavamura–Kuribayashi, H.; Koga, N.; Morokuma, K. J Am Chem Soc 1992, 114, 2359 and 8687; (b) Siegbahn, P. E. M. Chem Phys Lett 1993, 205, 290; (c) Axe, F. U.; Coffin, J. M. J Phys Chem 1994, 98, 2567.
14. Yoshida, T.; Koga, N.; Morokuma, K. Organometallics 1995, 14, 746.
15. (a) Woo, T. K.; Fan, L.; Ziegler, T. Organometallics 1994, 13, 2252; (b) Lorenz, J. C. W.; Woo, T. K.; Ziegler, T. J Am Chem Soc 1995, 117, 12793; (c) Lorenz, J. C. W.; Woo, T. K.; Fan, L.;

Ziegler, T. J. Organomet Chem 1995, 497, 91; (d) Cavallo, L.; Guerra, G. Macromolecules 1996, 29, 2729; (e) Woo, T. K.; Margl, P.; Ziegler, T.; Blöchl, P. E. Organometallics 1997, 16, 3454; (f) Margl, P.; Deng, L.; Ziegler, T. J Am Chem Soc 1999, 121, 154.

16. (a) Coles, M. P.; Jordan, R. F. J Am Chem Soc 1997, 119, 8125; (b) Coles, M. P.; Swenson, D. C.; Jordan, R. F.; Young, V. G., Jr. Organometallics 1997, 16, 5183.
17. (a) Ziegler, K.; Gellert, H.-G.; Zosel, K.; Holzkamp, E.; Schneider, J.; Söll, M.; Kroll, W.-R. Justus Liebigs Ann Chem 1960, 629, 121; (b) Martin, H.; Bretinger, H. Makromol Chem 1992, 193, 1283.
18. (a) Tsutsui, T.; Mizuno, A.; Kashiwa, N. Polymer 1989, 30, 428; (b) Jüngling, S.; Mülhaupt, R.; Stehling, U.; Brintzinger, H. H.; Fischer, D.; Langhauser, F. J Polym Sci Part A 1995, 33, 1305.
19. (a) Bunel, E.; Burger, B. J.; Bercaw, J. E. J Am Chem Soc 1988, 110, 976; (b) Resconi, L.; Waymouth, R. M. J Am Chem Soc 1990, 112, 4953; (c) Resconi, L.; Piemontesi, F.; Franciscono, G.; Abis, L.; Fiorani, T. J Am Chem Soc 1992, 114, 1025.
20. (a) Resconi, L.; Bossi, S.; Abis, L. Macromolecules 1990, 23, 4489; (b) Chien, J. C. W.; Wang, B. P. J Polym Sci, Part A 1990, 28, 15.
21. Vosko, S. H.; Wilk, L.; Nusair, M. Can J Phys 1980, 58, 1200.
22. (a) Becke, A. Phys Rev A 1988, 38, 3098; (b) Perdew, J. P. Phys Rev B 1986, 33, 8822.
23. (a) Lee, C.; Yang, W.; Parr, R. G. Phys Rev B 1988, 37, 785; (b) Becke, A. D. J Chem Phys 1993, 98, 1372; (c) Becke, A. D. J Chem Phys 1993, 98, 5648.
24. Møller, C.; Plesset, M. S. Phys Rev 1934, 46, 618.
25. Pople, J. A.; Binkley, J. S.; Seeger, R. Int J Quantum Chem 1976, 10, 1.
26. Krishnan, R.; Pople, J. A. J Chem Phys 1978, 14, 91.
27. Raghavachori, K.; Pople, J. A. Int J Quantum Chem 1981, 20, 1067.
28. (a) Purvis, G. D.; Bartlet, R. J. J Chem Phys 1982, 76, 1910; (b) Raghavachori, K.; Trucks, G. W.; Pople, J. A.; Head–Gordon, M. Chem Phys Lett 1989, 157, 479.
29. (a) Kestner, N. R. J Chem Phys 1968, 48, 252; (b) Liu, B.; McLean, A. D. J Chem Phys 1973, 59, 4557.
30. (a) For a review on the BSSE, see van Lenthe, J. H.; van Duijneveldt van de Rijdt, J. G. C. M.; van Duijneveldt, F. B. Adv Chem Phys 1987, 69, 521, and references therein; (b) van Duijneveldt, F. B.; van Duijneveldt van de Rijdt, J. G. C. M.; van Lenthe, J. H. Chem Rev 1994, 94, 1873; (c) van Duijneveldt, F. B. Molecular Interaction; Scheiner, S., Ed.; John Wiley & Sons Ltd: London, 1997.
31. Reinhold, M.; McGrady, J. E.; Meier, R. J. Chem Soc Dalton Trans 1999, 484.
32. Car, R.; Parrinello, M. Phys Rev Lett 1985, 55, 2471.
33. (a) Hariharan, P. C.; Pople, J. A. Theoret Chem Acta 1973, 28, 213; (b) Francl, M. C.; Petro, W. J.; Hehre, W. J.; Binkley, J. S.; Gordon, M. S.; Defrees, D. J.; Pople, J. A. J Chem Phys 1982, 77, 3654.
34. ADF 2.3.0; Theoretical Chemistry, Vrije Universiteit: Amsterdam; Baerends E. J.; Ellis, D. E.; Ros, P. Chem Phys 1973, 2, 24; te Velde, G.; Baerends, E. J. J Comp Phys 1992, 99, 84; Fonseca Guerra, C; et al. METECC-95 1995, 305.
35. Snijders, J. G.; Baerends, E. J.; Vernoijs, P. At Nucl Data Tables 1982, 26, 483.
36. Vernoijs, P.; Snijders, J. G.; Baerends, E. J. Slater Type Basis Functions for the Whole Periodic System; Department of Theoretical Chemistry, Free University: Amsterdam, 1994.
37. Krishnan, R.; Schlegel, H. B.; Pople, J. A. J Chem Phys 1980, 72, 4654; (b) Szabo, A.; Ostlund, N. S. Modern Quantum Chemistry: Introduction to Advanced Electronic Structure Theory; MacMillan Publishing Co., Inc.: New York, 1982.
38. GAMESS-U K Generalised Atomic and Molecular Electronic Structure System; Guest, M. F.; Fantucci, P.; Harrison, R. J. Kendrick, J.; van Lenthe, J. H.; Schoeffel, K.; Sherwood, P., Eds.; Daresbury Laboratory: Warrington, UK.
39. Frisch, M. J.; Trucks, G. W.; Schlegel, H. B., Gill, P. M. W.; Johnson, B. G.; Robb, M. A.; Cheeseman, J. R.; Keith, T.; Petersson, G. A.; Montgomery, J. A.; Raghavachari, K.; Al-Laham, M. A.; Zakrzewski, V. G.; Ortiz, J. V.; Foresman, J. B.; Cioslowski, J.; Stefanov, B. B.; Nanayakkara, A.; Challacombe, M.; Peng, C. Y.; Ayala, P. Y.; Chen, W.; Wong, M. W.; Andres, J. L.; Replogle, E. S.; Gomperts, R.; Martin, R. L.; Fox, D. J.; Binkley, J. S.; Defrees, D. J.; Baker, J.; Stewart, J. P.; Head–Gordon, M.; Gonzalez, C.; Pople, J. A. GAUSSIAN94; Gaussian, Inc.: Pittsburgh, PA, 1995.
40. Boys, S. F.; Bernardi, F. Mol Phys 1970, 19, 553.
41. (a) Brookhart, M.; Green, M. L. H. J Organomet Chem 1983, 250, 395; (b) Brookhart, M.; Green, M. L. H. J. Chem Soc Chem Commun 1983, 691.
42. Ziegler, T. Chem Rev 1991, 91, 651.
43. The size consistency correction for the CI calculation is quite large (≈40 kcal/mol) for the olefin complexation energy. Therefore, one can also expect significant errors in this correction, which will strongly affect the calculated correlation energy.
44. Machado, F. B. C.; Davidson, E. R. J Phys Chem 1993, 97, 4397.
45. Jensen, V.; Børve, K. J Comput Chem 1998, 19, 947.
46. Darwent, B. d. B. Bond Dissociation Energies in Simple Molecules; NSRDS-NBS 31: Washington, DC, 1970.
47. Burger, B., J.; Thompson, M. E.; Cotter, D.; Bercaw, J. E. J Am Chem Soc 1990, 112, 1566.
48. McQuarrie, D. A. Statistical Thermodynamics; Harper & Row: New York, 1973.
49. (a) Barone, V.; Adamo, C. J Chem Phys 1996, 105, 11007; (b) Barone, V.; Orlandini, L.; Adamo, C. Int J Quantum Chem 1995, 56, 691; (c) Barone, V.; Adamo, C. Chem Phys Lett 1994, 224, 432; (d) Latajka, Z.; Bouteiller, Y.; Scheiner, S. Chem Phys Lett 1995, 234, 159; (e) Jursic, B. J. Chem Soc Perkin Trans 1997, 2, 637.
50. Talarico, G.; Budzelaar, P. H. M.; Gal, A. W. Manuscript in preparation.